

COLLAPSE OF ACCRETING WHITE DWARF  
TO FORM A NEUTRON STAR

Ken'ichi Nomoto

Department of Physics  
Ibaraki University, Mito 310, Japan

Shigeki Miyaji

and

Daiichiro Sugimoto

Department of Earth Science and Astronomy  
College of General Education  
University of Tokyo, Tokyo 153, Japan

and

Koichi Yokoi

Science and Engineering Research Laboratory  
Waseda University, Tokyo 160, Japan

ABSTRACT

In a close binary system with a primary star in the mass range 8-12  $M_{\odot}$ , the primary star leaves a white dwarf composed of  $^{16}\text{O}$ ,  $^{20}\text{Ne}$ , and  $^{24}\text{Mg}$  as a result of mass exchange. When the companion star fills its Roche lobe, overflowing matter accretes onto the white dwarf. We have computed the evolution of such an accreting O-Ne-Mg white dwarf and found that electron captures on  $^{24}\text{Mg}$  and  $^{20}\text{Ne}$  trigger the collapse when the mass reaches 1.38  $M_{\odot}$ . As a result of the collapse, oxygen begins to deflagrate but the effects of electron captures dominate over the oxygen deflagration. The white dwarf collapses to form a neutron star.

## 1. FORMATION OF O-Ne-Mg WHITE DWARFS IN CLOSE BINARY SYSTEMS

In close binary systems, mass exchange between the component stars takes place. When a primary star is more massive than  $12 M_{\odot}$ , it leaves a helium star more massive than  $3 M_{\odot}$ . It evolves to form an iron core which collapses due to the photo-dissociation of iron nuclei. Whether the collapsing star leaves a neutron star or a black hole is still uncertain despite many investigations.

When the primary star is less massive than  $8 M_{\odot}$ , it leaves a white dwarf of helium or carbon plus oxygen. When the companion star evolves to fill its Roche lobe, overflowing matter accretes onto the white dwarf. The white dwarf experiences many cycles of hydrogen or helium shell flashes near its surface. Ultimately, helium detonation or carbon deflagration takes place in the central region (Nomoto and Sugimoto 1977; Nomoto et al. 1976), which disrupts the white dwarf completely. No remnant star is left.

Between these two types of evolution, there remains a mass range of  $8-12 M_{\odot}$ . Even for a single star, evolution of the star in this range is still left for detailed investigation except a preliminary report given by Barkat et al. (1974). By applying their results, we can construct the evolutionary scenario of such a close binary system as follows.

After the first mass exchange, the primary star leaves a helium star of  $2-3 M_{\odot}$ . In this star, a C+O core of mass around  $1.2 M_{\odot}$  is formed. Then the carbon burning takes place in a non-electron-degenerate condition. This implies that the helium envelope does not expand to a red giant size during these stages. However, electrons become degenerate in the resultant core of carbon burning products, i.e., in O-Ne-Mg core. Until the O-Ne-Mg core grows up to around  $1.2 M_{\odot}$ , copious neutrino loss from the carbon burning shell makes its evolution too rapid to expand the helium envelope appreciably. After that, however, the growth of the core mass is controlled by the helium shell burning, which makes the evolution slower. Eventually, the helium zone will expand to a red giant size and it overflows its Roche lobe as shown by Paczyński (1971) for the helium star of  $2 M_{\odot}$  having C+O core. After this mass exchange, the star will cool down and a O-Ne-Mg white dwarf will be left.

When the companion star evolves and comes to fill its Roche lobe, the mass accretes onto the O-Ne-Mg white dwarf. Unless all of the accreted material is ejected by a nova-like explosion, the mass of the white dwarf grows eventually up to the Chandrasekhar limit  $M_{Ch}$ .

In the present paper, we have computed the evolution of such an accreting O-Ne-Mg white dwarf. We have found that electron captures on  $^{24}\text{Mg}$  and  $^{20}\text{Ne}$  trigger the collapse when the mass reaches  $1.38 M_{\odot}$ . As a result of the collapse, oxygen begins to deflagrate but the effects of electron captures dominate over the oxygen deflagration. The white dwarf collapses to form a neutron star.

## 2. EFFECTS OF ELECTRON CAPTURES AND PHYSICAL DATA

Electron capture reactions in a strongly electron-degenerate condition cause three effects: (a) Decrease in the number of electrons and resultant decrease in pressure, (b) increase in the mean molecular weight of electrons  $\mu_e$  which leads to the decrease in  $M_{Ch}$  as  $\mu_e^{-2}$ , and (c) entropy production by secondary gamma-rays emitted from the excited states of the daughter nuclei and by the distortion in the electron distribution function.

The effects (a) and (b) trigger the collapse of the white dwarf, while the effect (c) and the compression of matter lead to ignition of oxygen. Competition between these effects determines the further evolution of the white dwarf. We have followed all these processes by numerical computation.

Rates of electron captures on  $^{15}\text{N}$ ,  $^{16}\text{N}$ ,  $^{16}\text{O}$ ,  $^{20}\text{F}$ ,  $^{20}\text{Ne}$ ,  $^{24}\text{Na}$ , and  $^{24}\text{Mg}$  and associated neutrino losses were computed mainly with the help of the gross theory of  $\beta$ -decay (Egawa et al. 1975). For electron captures on nuclei in nuclear statistical equilibrium (NSE), we used a table given by Yokoi et al. (1979) which was prepared on the basis of Mazurek's data (1973). Other physical data and method of computation are the same as those used by Nomoto and Sugimoto (1977).

## 3. EVOLUTION AND COLLAPSE OF THE ACCRETING O-Ne-Mg WHITE DWARF

Evolutionary aspects are displayed in Fig. 1-3 against the central density  $\rho_c$  of the white dwarf. In Fig. 1, the change in the central temperature  $T_c$  is shown and stages where electron captures take place are indicated. In Fig. 2, are shown changes in the time scale of the gravitational contraction/collapse, i.e.,  $\tau_\rho \equiv dt/d\ln\rho_c$ , the energy generation rate  $L_{O+O}$  by oxygen burning, the rate of energy absorption by dissociation of nuclei into lighter ones  $L_{NSE}$ , and the neutrino luminosity  $L_\nu$ . Changes in the radial distances  $\underline{r}$  of the Lagrangian shells are shown in Fig. 3. We found that the accreting white dwarf evolves through the following phases.

(1) Growth of the mass by accretion: As the mass  $M$  approaches the Chandrasekhar limit, the central density increases. The time scale is determined by the accretion rate. We applied the accretion rate of  $dM/dt = 4 \times 10^{-6} M_\odot \text{yr}^{-1}$ , which corresponds to a core immersed deep in the red giant envelope. However, this result can be applied also to the case of much slower accretion onto the white dwarf.

(2) Electron capture on  $^{24}\text{Mg}$ : This reaction takes place when  $\rho_c$  exceeds the corresponding threshold density at #2 in Fig. 1. The resultant  $^{24}\text{Na}$  also captures an electron after #3. These reactions produce much heat, mainly by gamma-ray emissions. Temperature rises, and a convective core appears as shown by the curled region in Fig. 3. It extends to  $M_r = 0.6 M_\odot$  and fresh  $^{24}\text{Mg}$  is mixed into the convective core. Then,  $\mu_e$  increases gradually over the convective core. This results in appreciable decrease of  $M_{Ch}$ . Consequently,  $\tau_\rho$  becomes shorter and shorter as seen in Fig. 2.

(3) Electron capture on  $^{20}\text{Ne}$ : This reaction becomes rapid at #4 and the resultant  $^{20}\text{F}$  captures another electron immediately. At this time, the value of  $M_{\text{Ch}}$  has already become almost equal to the white dwarf mass. Consequently, the contraction is well quasi-dynamic as seen in the values  $\tau_{\rho}$  in Fig. 2.

(4) Initiation of Oxygen Deflagration: During the quasi-dynamic collapse, the temperature in the central region rises, mainly due to the compression as seen in Fig. 1. When  $\rho_{\text{C}}$  reaches  $2.5 \times 10^{10} \text{g cm}^{-3}$ , the oxygen burning becomes rapid (#5) and grows into a deflagration (#6). However, it does not grow into a detonation wave at all, because the nuclear energy release is only five percent of the internal energy in the central region of the white dwarf (cf. Nomoto et al. 1976).

(5) Competition between oxygen deflagration and electron captures: The deflagration front (DF) propagates outward in mass and processes the core material into the composition of nuclear statistical equilibrium (NSE) (#6 - #8). Nuclear energy generation rate at the DF amounts to  $L_{0+0} \approx 10^{18} L_{\odot}$  at #8. However, almost the same amount of energy is absorbed in the NSE core as shown by  $-L_{\text{NSE}}$  in Fig. 2, because the nuclei are dissolved into lighter ones during the collapse. From #6 through #8, the total energy of the white dwarf decreases by  $3 \times 10^{50}$  erg via the neutrino emission accompanied with electron captures. Therefore the white dwarf will continue to collapse (Fig. 3).

(6) Formation of a neutron star: Though we stopped computing at #8, the collapse will make a bounce around nuclear density because even an iron core of  $1.4 M_{\odot}$  does so (Arnett 1977). Our bounced star will not collapse into a black hole any more but remain to be a neutron star, because even the total mass of the star is as small as  $1.38 M_{\odot}$ , smaller than the limiting mass of the neutron star.

#### REFERENCES

- Arnett, W.D. 1977, *Ap. J.*, 218, 815.  
Barkat, Z., Reiss, Y., and Rakavy, G. 1974, *Ap. J. (Letters)*, 193, L21.  
Egawa, Y., Yokoi, K., and Yamada, M. 1975, *Prog. Theor. Phys.*, 54, 1339.  
Mazurek, T.J. 1973, Ph. D. Thesis, Yeshiva Univ.  
Paczynski, B. 1971, *Acta Astron.*, 21, 1.  
Nomoto, K., and Sugimono, D. 1977, *Publ. Astron. Soc. Japan*, 29, 765  
Nomoto, K., Sugimoto, D., and Neo, S. 1976, *Astrophys. Space Sci.*, 39, L37.  
Yokoi, K., Neo, S., and Nomoto, K. 1979, *Astron. Astrophys.*, in press.

Fig. 1. Evolutionary changes in the central density and temperature of the accreting O-Ne-Mg white dwarf. Vertical lines indicate the threshold densities for electron captures on  $^{24}\text{Mg}$ ,  $^{20}\text{Ne}$ , etc. Time scale of temperature rise due to oxygen burning  $\tau_N(0)$  is equal to free-fall time scale  $\tau_{ff}$  at the dashed line.

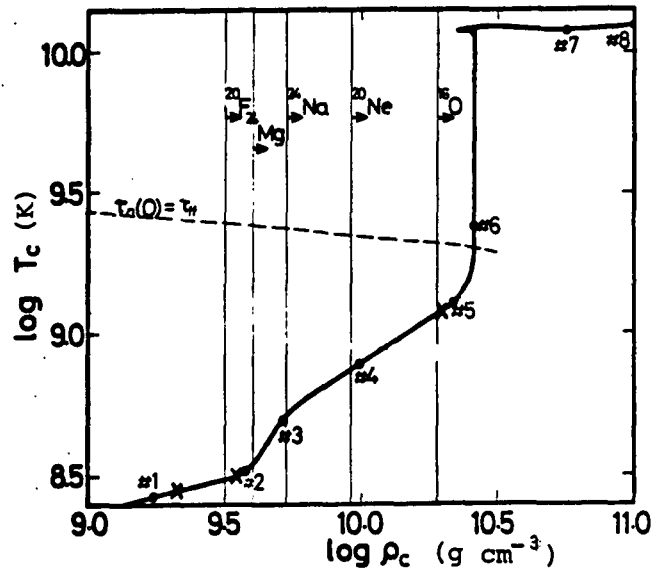


Fig. 2. Changes in time scales of collapse  $\tau_p$  and free-fall  $\tau_{ff}$  against the central density. Also shown are the energy generation rate by oxygen burning  $L_{O+O}$ , the rate of energy absorption in the NSE region  $L_{NSE}$ . These two almost cancel each other from #6 through #8.  $L_\nu$  is the neutrino luminosity.

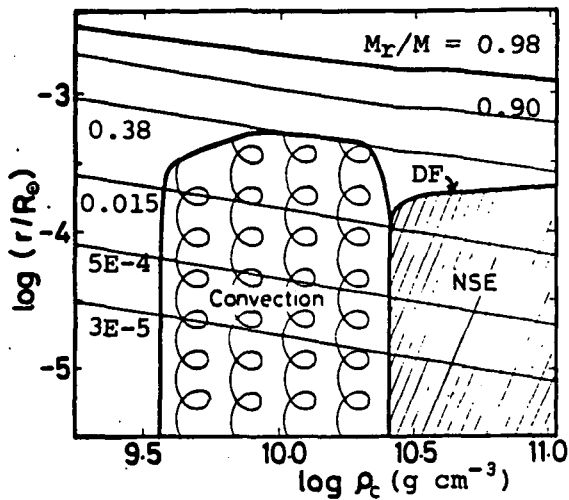
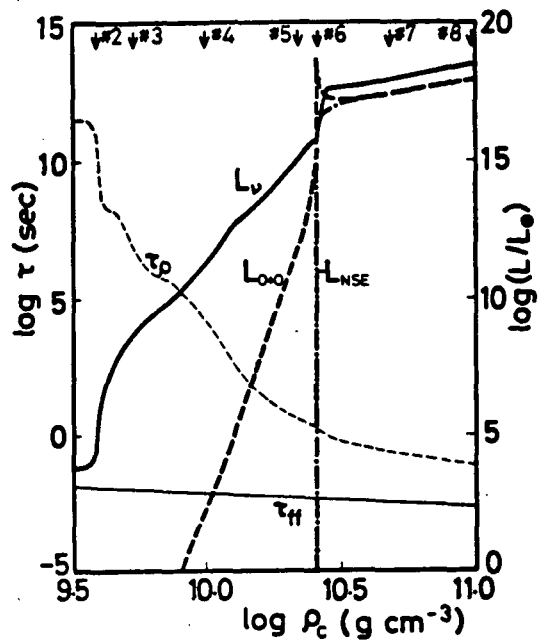


Fig. 3. Changes in the radial distance  $r$  of the Lagrangian shell for which  $M_r/M$  is indicated. DF indicates the position of the oxygen-deflagration front.